

Proteomic Profiling in *Pediococcus pentosaceus* SF11 Exposed to Condensed Tannins from Sainfoin

Rongzheng Huang, Fanfan Zhang, Xuzhe Wang, Fan Yang, and Chunhui Ma*



Cite This: *ACS Omega* 2024, 9, 41148–41156



Read Online

ACCESS |



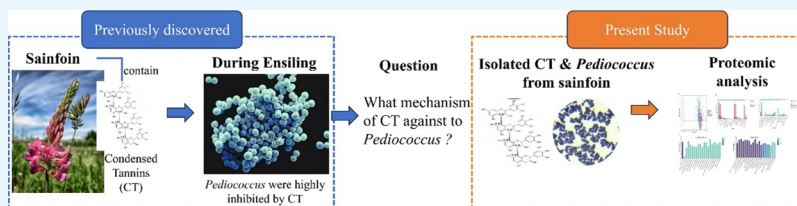
Metrics & More



Article Recommendations



Supporting Information



ABSTRACT: The antibacterial mechanism of condensed tannins (CTs) obtained from tea has been elucidated, but the mechanism of legume-derived CTs remains unclear. The mechanisms of legume- and tea-derived CTs probably differ due to the diverse compositions of CTs. Previous research found that sainfoin CTs directly inhibited the growth of *Pediococcus*. The present study investigated the inhibition mechanism of CTs against *Pediococcus pentosaceus* SF11 (SF11) through proteomic analysis. The results showed that the minimum inhibitory concentration (MIC) of CTs against SF11 was 1500 mg/L and that CTs increased cell membrane permeability in a dose-dependent manner. In total, 418 differentially expressed proteins (DEPs) were identified between the CT treatment and the control, among which 341 were down-regulated and 77 were up-regulated in the CT treatment. The protein interaction network showed that the expression of only two DEPs was highly different between CT treated and control ($|\log_2FC| > 2$); the *atpD* protein was up-regulated in the CT-treated group, which was involved in ATP synthesis; down-regulated DEPs were most involved in lipoteichoic acid synthesis, peptidoglycan synthesis, and glycine metabolism. Twenty-seven proteins were not detected after CT treatment, which were involved in functions including fatty acid synthesis, RNA synthesis and translation, drug resistance, and cell membrane permeability in SF11. Therefore, the findings suggest that the inhibition mechanism of CTs may be related to cell membrane damage and inhibition of cell reproduction.

1. INTRODUCTION

Pediococcus pentosaceus is a Gram-positive bacteria that belongs to the homofermentative lactic acid bacteria (LAB) with facultative anaerobic and carbohydrate degradation features.¹ *P. pentosaceus* is harmless in biological applications and is widely used in food engineering, agriculture, and animal husbandry due to its functional characteristics, such as its bacteriostatic capacity, antifungal ability, bacteriocin production, anti-inflammatory activity, anticarcinogenic properties, and promotion of mineral and nutrient utilization.² These functions of *P. pentosaceus* are activated through fermentation processes. A previous study observed that the abundance of *Pediococcus* was directly inhibited by condensed tannins (CTs) during the fermentation of sainfoin silage.³

CTs are secondary plant metabolites composed of diverse mixtures of oligomeric and polymeric substances including flavan-3-ols. Catechin (C), epicatechin (EC), gallocatechin (GC), epigallocatechin (EGC), epicatechin gallate (ECG), gallocatechin gallate (GCG), and epigallocatechin gallate (EGCG) are the subunits of CTs and are widely distributed in grass and legumes.⁴ Therefore, inhibition due to CTs is likely to have an enormous impact on the utilization of *P. pentosaceus* in animal husbandry. The biological activity of CTs

shows correlations with the presence of galloyl and gallic moieties in the flavan-3-ol units. Among them, EGCG has captured the most interest from microbiology scientists because it has both galloyl and gallic moieties in flavan-3-ol units, resulting in the highest inhibitory activity against bacteria.⁵ The antibacterial mechanism of CTs from green tea has been thoroughly investigated.⁶ However, few studies have focused on the antibacterial activity of CTs from legumes. Various legume plants, such as sainfoin, contain CTs, which have a different composition of flavan-3-ols compared to those from green tea.⁴ Considering the different composition of CTs obtained from green tea and sainfoin CTs, which lack EGCG subunits, in this study, it was hypothesized that the antibacterial capacity of sainfoin CTs would be lower than that of EGCG and the antibacterial mechanism would be different. The present study aimed to elucidate the inhibition

Received: November 24, 2023

Revised: August 26, 2024

Accepted: September 6, 2024

Published: September 23, 2024



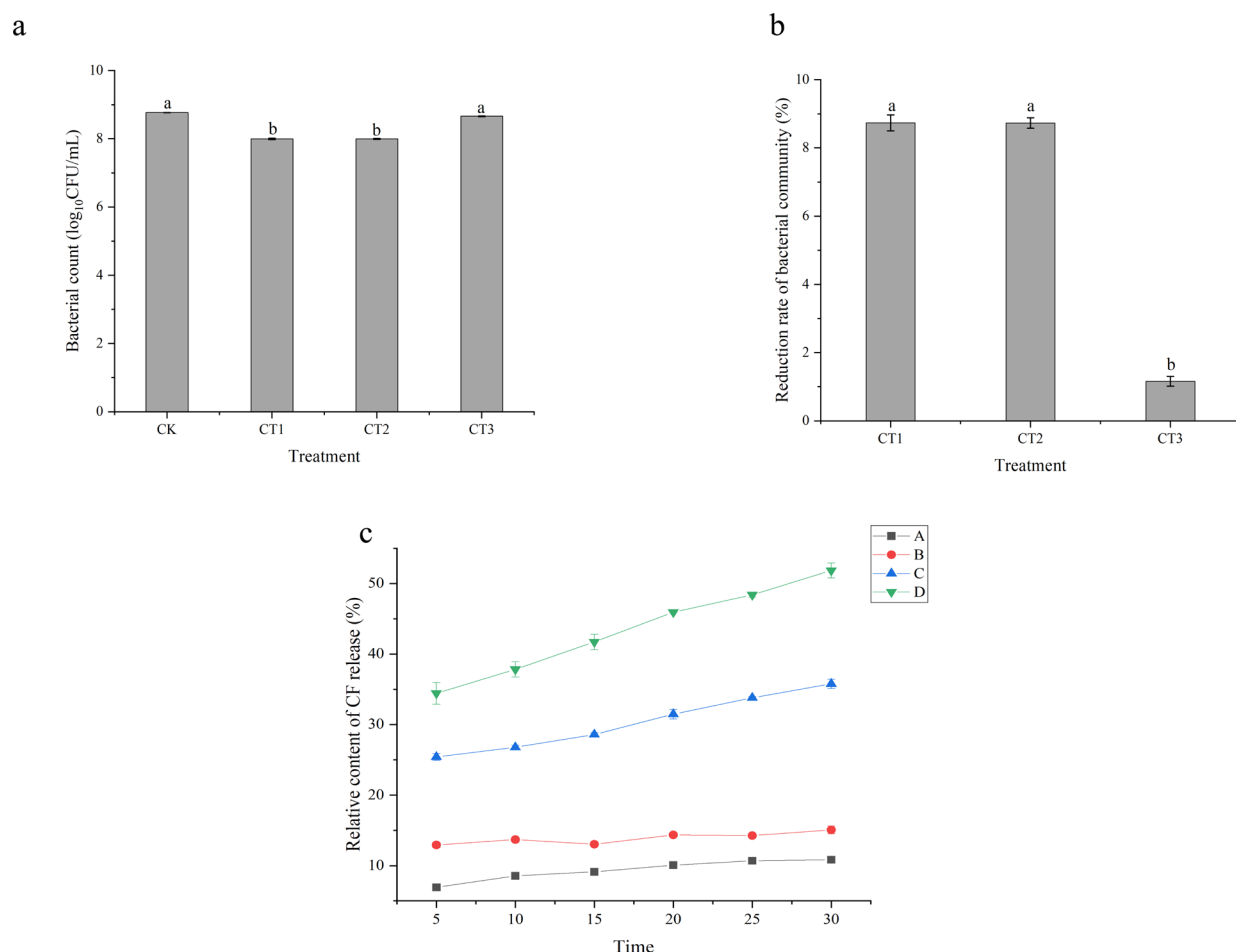


Figure 1. Growth of *P. pentosaceus* SF11 under different concentrations of CTs after 8 h of incubation. (a) Bacterial count. (b) Reduction rate of the bacterial community. (c) CF release rate. CK: control. CT1, CT2, and CT3: addition of CTs at 1500, 750, and 375 mg/L, respectively. A, B, C, and D: addition of CT at 200, 500, 1000, and 1500 mg/L, respectively.

mechanism of sainfoin CTs on *P. pentosaceus* at the proteomic level.

2. MATERIALS AND METHODS

2.1. Strain and CTs. CTs were extracted from sainfoin, and *P. pentosaceus* strain SF11 was isolated from sainfoin silage after 7 or 14 days of fermentation. The sequence of strain SF11 was uploaded to the National Center for Biotechnology Information (NCBI) under number “ON866519” (accessed on July 3, 2022). The procedures used for strain isolation and CT extraction can be found in the [Supporting Information](#).

2.2. Strain Growth under CT Conditions. According to previously described methods,⁷ 100 μ L of CTs with different concentrations of 1 \times minimum inhibitory concentration (MIC), 0.5 \times MIC, and 0.25 \times MIC were added to 850 μ L of bacterial solution at a concentration of approximately 1×10^6 colony-forming units (CFU)/mL, and incubation was performed for 8 h at 37 $^{\circ}$ C. After incubation, 100 μ L of bacteria solution was added to MRS agar and incubated for 24 h at 37 $^{\circ}$ C. The microbial data concentrations were presented as log-transformed before statistical analysis.

All reagents described below were purchased from Sigma-Aldrich Co., Ltd., Berlin, Germany, unless otherwise specified.

2.3. Determination of the MIC of CTs. The broth dilution method⁸ was used to determine the MIC of CTs against *P. pentosaceus* SF11. Briefly, CTs were diluted to 125–

3000 mg/L after filter membrane sterilization (aperture, 0.45 μ m). One milliliter of bacterial solution (MRS broth with SF11 growth for 3.5–4 h) was taken, and the concentration was diluted to 106 CFU/mL. Next, 50 μ L of bacteria solution with and without the addition of 50 μ L of CT solution was added to 96 microporous plates (the final concentration of the bacteria was approximately 5×10^5 CFU/mL), followed by incubation at 37 $^{\circ}$ C for 24 h.

2.4. Effect of CTs on the Intracellular Protease of *P. pentosaceus* SF11. The bacterial solution was adjusted to OD₆₀₀ = 0.5 ($\sim 10^8$ CFU/mL) after overnight culture.⁹ Then, bacteria were cultured on MRS broth with or without the addition of 1500 mg/L CTs for 2, 6, 10, and 24 h. Cells were harvested following centrifugation at 8000 rpm for 5 min and washed twice with 0.1 M phosphate-buffered saline (PBS) solution (pH = 7.0). Cells were broken according to previously described methods,¹⁰ and the supernatant was collected for protease activity analysis. The protein content of the bacterial solution was determined according to previously reported methods (Bradford, 1976).¹¹ To determine the activity of 1-deoxy-D-xylulose 5-phosphate reductoisomerase (DRX),¹² 1-deoxy-D-xylulose 5-phosphate (DXP) was used as a substrate and the change in absorbance at 340 nm was measured.

The β -ketoacyl-ACP reductase (FabG) activity was determined by using the FabG assay kit (Elabscience Biotechnology Co., Ltd., Wuhan, China). Purified FabG

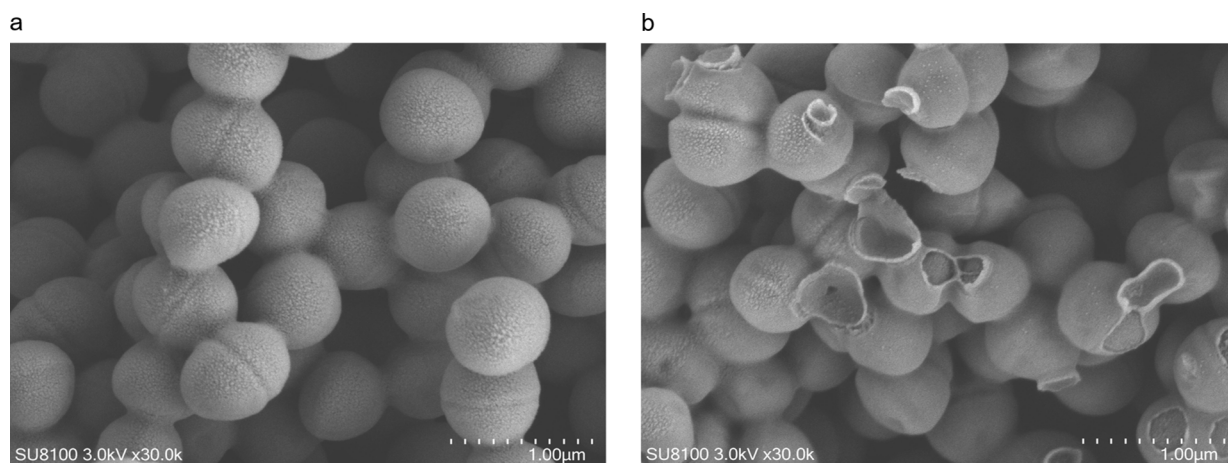


Figure 2. Scanning electron microscopy (SEM) images showing the effects of CTs on the cell morphology of *P. pentosaceus* SF11. (a) Control. (b) CT-treated (750 mg/L).

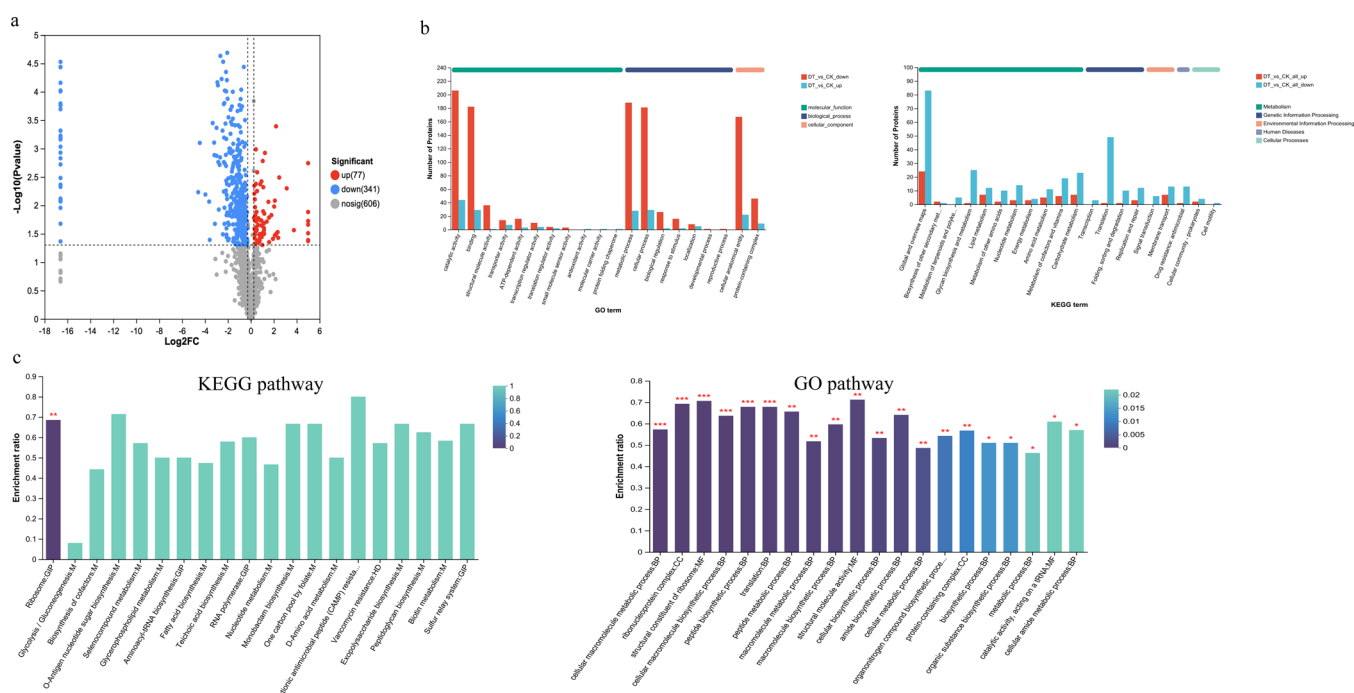


Figure 3. (a) Volcano plot analysis, (b) Gene Ontology (GO) and Kyoto Encyclopedia of Genes and Genomes (KEGG) annotation, and (c) KEGG and GO enrichment point map analysis of *P. pentosaceus* SF11 with and without the addition of CTs. CK: control; DT: CT-treated (750 mg/L).

obtained from *Escherichia coli* was used as a solid-phase antibody. FabG was extracted and purified from *E. coli* according to the methods described above.^{13,14}

2.5. Scanning Electron Microscopic Analysis. Bacteria was cultured on the MRS broth with or without the addition of CTs at a concentration at 750 mg/L for 8 h at 37 °C. The bacterial cells were collected after centrifugation (8000 rpm, 5 min), and 0.1 M PBS (pH = 7.0) was used to wash the obtained cells twice. Fixation and dehydration of bacteria was followed by suitable methods.^{15,16} The cell morphology of bacteria was analyzed using a scanning electron microscope (SU8100, Hitachi Co., Ltd., Tokyo, Japan.).

2.6. Determination of Cell Membrane Permeability. According to previously described methods,^{17,18} 5,6-carboxy-fluorescein (CF) was used as a fluorescent probe. Phosphatidylcholine (PC) liposomes containing 100 mM CF were

introduced into the liposomes using ultrasound. The liposomes were passed through a Sepharose CL-4B column, and the effluent was collected. The total CF content of the liposomes was determined through the addition of 0.2% Triton X-100 to the solution. The CF content of the solution was determined after the addition of CTs at different concentrations (200, 500, 1000, and 1500 mg/L). The fluorescence intensity of the liposome solution was determined at Ex 320/Em 510 nm by using the Synergy 2 detector (BioTek Instruments, Inc., USA).

2.7. Proteomic Analysis. The bacterial solution was adjusted to OD₆₀₀ = 0.5 (~10⁸ CFU/mL) after overnight culture. Then, bacteria were cultured on the MRS broth with or without the addition of CTs at a concentration of 750 mg/L for 7 h. The cells were collected after centrifugation (8000 rpm, 5 min) and washed twice using 0.1 M PBS (pH = 7.0). Samples were subjected to analysis with the 4D-label-free

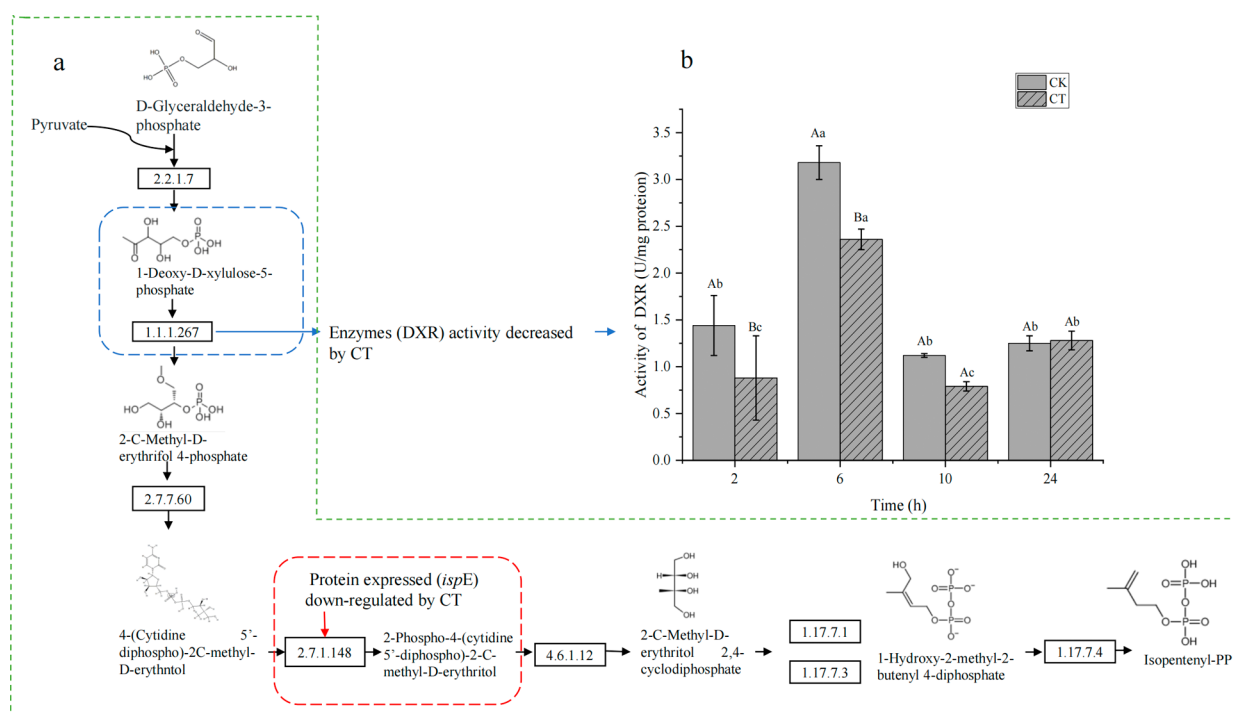


Figure 4. (a) DEPs involved in 2-C-methyl-D-erythritol 4-phosphate (MEP) pathways and (b) activity of DXR in *P. pentosaceus* SF11 with and without the addition of CTs (1500 mg/L, 24 h incubation). 2.2.1.7:1-deoxy-D-xylulose-5-phosphate synthase (dxs); 1.1.1.267:1-deoxy-D-xylulose-5-phosphate reductoisomerase (DXR); 2.7.7.60:2-C-methyl-D-erythritol 4-phosphate cytidyltransferase (*ispD*); 2.7.1.148:4-diphosphocytidyl-2-C-methyl-D-erythritol kinase (*ispE*); 4.6.1.12:2-C-methyl-D-erythritol 2,4-cyclodiphosphate synthase (*ispF*); 1.17.7.1/1.17.7.3: (*E*)-4-hydroxy-3-methylbut-2-enyl-diphosphate synthase (*gcpE/ispG*); and 1.17.7.4:4-hydroxy-3-methylbut-2-en-1-yl diphosphate reductase (*ispH*).

method and liquid chromatography–tandem mass spectrometry (LC-MS/MS) at Majorbio Co., Ltd. (Shanghai, China). The procedures used for protein extraction, protein reductive alkylation and digestion, peptide desalination and quantification, LC-MS/MS analysis, and sequence database searches can be found in the [Supporting Information](#).

The data were subjected to Student's *t* test, and differences were considered significant at $p < 0.05$. Proteins with >1.2 (up-regulated)- or <0.83 (down-regulated)-fold change (FC) in abundance with $p < 0.05$ were regarded as differentially expressed proteins (DEPs).¹⁹

The parallel reaction monitoring (PRM) analysis was used to validate the DEPs (20 proteins were selected), and specific methods can be found in the [Supporting Information](#).

2.8. Statistical Analysis. The characteristic data of *P. pentosaceus* SF11 with and without CTs were subjected to a one-way analysis of variance using a one (treatment) complete randomized design. Data were analyzed using IBM SPSS 22 Statistics (IBM Corp., Armonk, NY, USA). Significant differences between treatments were determined using Tukey's test at $p < 0.05$.

3. RESULTS

3.1. Effects of CTs on *P. pentosaceus* SF11. As shown in [Figure 1a](#), the addition of CTs (mainly contain EGC and GC, [Table S1](#)) at 750 and 1500 mg/L resulted in a lower bacterial count compared with the control ($p < 0.05$). The CT1 (1500 mg/L CTs) and CT2 (750 mg/L CTs) treatments showed no difference in the reduction rate of the bacterial community ($p > 0.05$), and the reduction rates of both were higher than in the CT3 treatment (375 mg/L CTs) ([Figure 1 b](#), $p < 0.05$).

The relative content of CF released increased as the CT concentration increased ([Figure 1c](#)).

As shown in [Figure 2 a and b](#), the cell wall of *P. pentosaceus* SF11 showed clear damage after CTs treatment, but cells still exhibited coccus-like shapes.

3.2. Proteomic Profiling of *P. pentosaceus* SF11. A total of 418 DEPs were identified ($p < 0.05$), among which 341 proteins were down-regulated and 77 were up-regulated under CT treatment compared with the control ([Figure 3 a](#), $p < 0.05$).

Among the DEPs, 347 DEPs were involved in the molecular function category, 249 DEPs were involved in the biological process category, and 207 DEPs were involved in the cellular component category ([Figure 3 b](#)). For molecular function, most DEPs were associated with catalytic activity (206 down-regulated and 44 up-regulated DEPs), followed by binding (182 down-regulated and 29 up-regulated). For biological processes, most DEPs were associated with metabolic processes (188 down-regulated and 28 up-regulated), followed by cellular processes (181 down-regulated and 29 up-regulated). For the cellular component category, most DEPs were associated with a cellular anatomical entity (167 down-regulated and 22 up-regulated), followed by the protein-containing complex (46 down-regulated and 9 up-regulated).

Based on KEGG and GO pathway annotation, the most significant enrichment protein was found involved in the ribosome pathway ([Figure 3c](#), $p < 0.05$). Based on the interaction network of proteins ([Figure S1](#)), only two DEPs (PEPE_RS07720 and PEPE_RS02390) showed higher FC values under CT treatment ([Table S2](#), $\log_2\text{FCI} > 2$); top 30 of these DEPs were involved in lipoteichoic acid (LTA) synthesis (PEPE_RS01815, down-regulated, [Figure S2a](#)), peptidoglycan

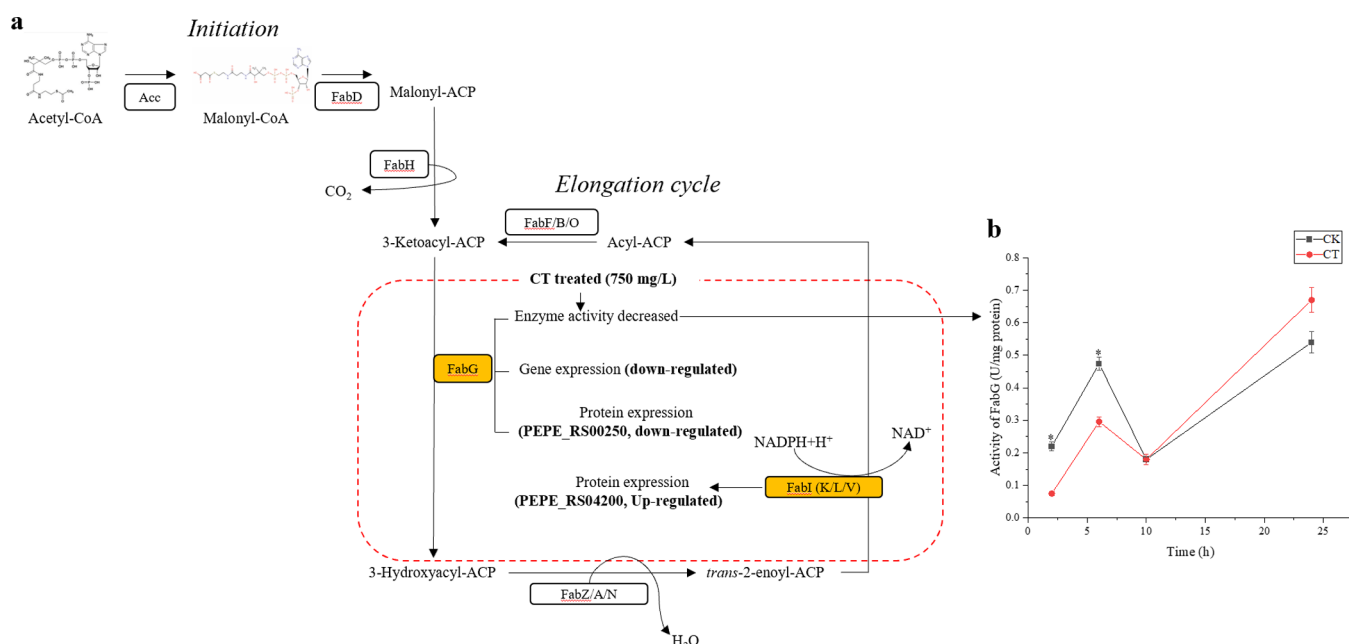


Figure 5. (a) DEPs involved in fatty acid biosynthesis and (b) activity of FabG in *P. pentosaceus* SF11 with and without the addition of CTs (1500 mg/L, 24 h incubation). CTs: condensed tannins, CK: control.

synthesis (PEPE_RS07584 and PEPE_RS01445, down-regulated, Figure S2b), ATP synthesis (PEPE_RS06385, up-regulated, Figure S2c), and glycine metabolism (PEPE_RS06435, down-regulated, Figure S2d). For ATP synthesis, the intracellular content of ATP in the cell were lower in CT treated compared with the control (Figure S3, $p < 0.05$). For glycine metabolism, the activity of dihydrofolate reductase (DHFR) was not significantly different between CT treated and control (Figure S4, $p > 0.05$).

As shown in Table S4, the 27 proteins were not detected in the CT-treated group compared with the control, which were involved in functions including fatty acid synthesis (such as *fabG*), isopentenyl pyrophosphate (IPP) synthesis (such as *ispE* and *dxr*), RNA synthesis and translation (such as *miaA*), drug resistance (such as *msrC*), and cell membrane permeability (such as *aqpZ*). The enzyme (2.7.1.148) expressed by *ispE* was down-regulated in the CT-treated group (Figure 4 a). The activity of DRX was highest in both the control and CT-treated groups after 6 h of incubation ($p < 0.05$). The CT-treated group showed lower activity compared with the control after 2 and 6 h of incubation ($p < 0.05$), as shown in Figure 4 b. The enzyme (FabG) expressed by *fabG* was down-regulated, while the expression of FabI (*fabI*) was up-regulated in the CT-treated group (Figure 5a). The activity of FabG increased with prolonged incubation time in both groups; however, the CT-treated group showed lower activity after 2 and 6 h of incubation compared with the control group ($p < 0.05$), as shown in Figure 5b.

4. DISCUSSION

4.1. Effect of CTs on *P. pentosaceus* SF11. The MIC of CTs against *P. pentosaceus* SF11 was 1500 mg/L. Under exposure to CTs at the MIC level, after incubation overnight, the bacterial community was reduced by 8%. Compared with EGCG, which showed bactericidal activities of over 99% against a broad variety of bacteria, such as *E. coli*, *Bordetella bronchiceptica*, and *Staphylococcus aureus*,⁷ the present results

indicated that CTs from sainfoin exhibited bacteriostatic activity. CTs damaged the cell walls of *P. pentosaceus* SF11, but cells were still integrated. Similar results were observed in *P. pentosaceus* under acid stress.¹⁹ The findings of the present study indicated that CT exposure probably exerted the same effect as acid stress on *P. pentosaceus* at the cell morphology level.

EGCG and EC obtained from green tea have the capacity to damage the liposome membrane, and EGCG causes the highest degree of membrane damage.¹⁸ Similar results were observed in this study; CTs showed a dose-dependent impact on the release of CF, indicating that the level of membrane damage was dependent on the CTs concentration. The affinity between EGCG and the bacterial cell membrane is higher than that between EGC and the cell membrane. EGCG can enter the bimolecular center position, while EGC remains on the surface of the molecular layer, indicating that EGCG has the greatest ability to disturb the cell membrane.²⁰ The CTs obtained from sainfoin were mainly composed of EGC (>65%, Table S1). Over 50% of the CF content was released after exposure to CTs at a concentration of 1500 mg/L. However, only 606 mg/L of EGCG could achieve the same effect.¹⁸ The results of the present study suggest that the capacity of sainfoin-derived CTs to damage the cell membrane is between those of EC and EGCG.

4.2. Proteomic Profiling of *P. pentosaceus* SF11 under CT Conditions. A total of 418 DEPs were identified; most of these were related to catalytic activity, followed by metabolic process, binding, cellular process, and cellular anatomical entity. Only the ribosome pathway was obviously enriched, and 11.28% DEPs (37) were involved in this pathway. All proteins related to the ribosome were found to be down-regulated under acetic acid stress in bacteria such as *Pediococcus acidilactici*¹⁹ and *Ethanoligenens harbinense*,²¹ and the ribosome was not the only pathway involved in acetic acid stress. However, the present results showed that one protein (*rplL*) was up-regulated in the ribosome pathway. These

results probably suggested that bacteria showed a weaker response to sainfoin CTs stress than acetic acid stress.

For important proteins which are involved in the network of interaction, only two DEPs (PEPE_RS07720 and PEPE_RS02390) expression were highly affected by CT. The results probably suggest that the expression of most important proteins is not strongly influenced by CTs, which could partly explain why CTs act in a bacteriostatic role rather than a bactericidal role. Among the down-regulated DEPs, the PEPE_RS01815 protein is a phosphoglycerol transferase that is involved in the last step of LTA synthesis. Polyanionic teichoic acids (TAs) are composed of wall teichoic acids (WTAs) and LTAs. Together with peptidoglycan, WTAs and LTAs make up a polyanionic network or matrix that provides several functions, such as assisting in material transportation.²² The PEPE_RS01445 (*glmU*) protein catalyzes the formation of GlcNAc-1P from D-GlcN-1P, and PEPE_RS07585 (*murF*) catalyzes the final step in the synthesis of murein from UDP-MurNAc. Both GlcNAc-1P and UDP-MurNAc are required for linkage unit synthesis, and the linkage unit (Gro-P)₂ or ₃ManNAc (β 1–4) GlcNAc-P to C-6 of the MurNAc residues is the basic unit for the attachment between WTA and peptidoglycan.²³ In addition, among the top 30 DEPs, the DEP with the highest FC was DltB, coded by PEPE_RS07720 (down-regulated, log₂ FC = –16.10), which is a D-alanyl-lipoteichoic acid biosynthesis protein. This D-alanyl carrier protein transfers the D-ala onto membrane-associated LTAs and WTAs for alanylation.²² Therefore, based on SEM results, CTs caused heavy damage to the cell wall though the decreased expression of proteins involved in LTA and WTA synthesis, especially for the alanylation of TA. The down-regulation of the PEPE_RS0645 protein (encoded by *glyA* and described as a serine hydroxymethyltransferase), which is involved in glycine metabolism, catalyzed the reversible interconversion of glycine with tetrahydrofolate (THF) serving as the one-carbon carrier, resulting in the production of 5,10-methylene-THF. Methylene-THF can generate methyl- or formyl-group donors to produce methionine and purines, and causes formylation of the amino acid attached to the initiator tRNA^{Met}, which is important for transition initiation.²⁴ In addition, the catalytic reduction of dihydrofolate (DHF) to THF through DHFR utilizes NADH as a cofactor, making DHFR a key enzyme involved in the transfer of one carbon unit of a cell, especially for the synthesis of purines and pyrimidines.⁶ Some strains of *Pediococcus* have shown DHFR activity.²⁵ Theoretically, EGCG is structurally analogous (at the A, C, and D rings) to common DHFR inhibitors such as methotrexate (MTX) and tetrahydroquinazoline (TQD), but the galloyl group (B ring) is not involved in the inhibition of DHFR.⁶ EGC and EC (both with and without gallic groups) extracted from green tea showed no effects on DHFR activity of the cell from bovine liver and human.^{26,27} The results indicate that the gallic group (D ring) must be the key factor underlying the inhibitory effects in animal cells. However, EC and C (both without and with gallic groups) both showed inhibitory effects on the DHFR of human cells, which was 2-fold compared to the inhibition ability of EGCG.²⁸ This difference was probably due to the different spatial structures of CTs obtained from different plants.⁴ Which group of CTs is involved in inhibitory activity against this enzyme needs further study. CTs showed antimicrobial activity through the hydrogen bond by hydroxyl groups and amino acid residue sites in proteins, such as Glu 30.²⁶ EGCG shows greater inhibitory

activity against DHFR in bacteria than in animals.²⁸ In the present study, CTs showed no effect on DHFR activity during the entire incubation period, which was partly related to the lack of EGCG in CTs derived from sainfoin. Therefore, the results of the present study suggested that CTs could impact the translation apparatus such as translation factors and the composition of the ribosome due to the inhibition of one-carbon metabolism through decreased enzyme expression. The RpoC protein coded by PEPE_RS06910 involved in RNA synthesis is described as a DNA-directed RNA polymerase subunit beta. The *rpoC* gene is located in highly conserved chromosomal regions of *Pediococcus* spp.²⁹ The results suggested that CTs decreased RNA synthesis through relative decreases in enzyme expression. The AtpD protein coded by PEPE_RS06385, which was up-regulated in the CT-treated group, is involved in ATP synthesis. The intracellular ATP content of *P. pentosaceus* SF11 decreased after the addition of CTs. CTs obtained from the rice straw showed the ability to decrease the ATP content of *S. aureus*, which indicated that the overall metabolic energy was reduced.³⁰ Thus, the up-regulated AtpD protein mainly occurred in response to the decreased intracellular ATP, which was attributed to the impact of CTs.

There were 27 proteins that were not detected due to CT impact, which were involved in functions, including fatty acid synthesis, RNA synthesis and translation, drug resistance, and cell membrane permeability. The IspE protein coded by PEPE_RS01335 is involved in the 2-C-methyl-D-erythritol 4-phosphate (MEP) pathway and is described as a 4-(cytidine 5'-diphospho)-2-C-methyl-D-erythritol kinase. The MEP pathway is only found in bacteria and mainly synthesizes isopentenyl pyrophosphate (IPP) as a terpene precursor.³¹ DRX is a rate-limiting enzyme involved in the MEP pathway.⁶ Researchers first observed DRX in *E. coli*. This enzyme uses NADPH as the sole coenzyme and requires metal ions such as magnesium to undergo reactions.³² The genes (*dxx*) encoding DRX enzymes have been discovered in over 20 bacteria, including *Bacillus subtilis* and *Pseudomonas aeruginosa*.³³ CTs showed a competitive inhibition mechanism for DRX but noncompetitive inhibition for NADPH.^{1,34} The present study found that CTs decreased the activity of DRX by 38.89 and 25.78% after 2 and 6 h of incubation, respectively, but had no inhibitory effects on DRX with a prolonged incubation time. Thus, CTs could inhibit the MEP pathway metabolism through directly decreasing enzyme activity and reducing enzyme expression in *P. pentosaceus* SF11. FabG, coded by PEPE_RS00250, is involved in fatty acid biosynthesis. FabG is widely distributed in bacteria and is a key rate-limiting enzyme for fatty acid synthesis, and the structure and active center of this enzyme show high similarity among different bacterial species (Oppermann et al.). The inhibition of FabG activity results in the obstruction of bacterial synthesis systems such as quorum sensing, cell membrane, and cell wall systems (Renzetti et al.⁶). The addition of a low concentration (<100 μ mol/L) of EGCG had a lag effect (40 min) on inhibiting FabG activity, resulting in a 10% decrease in the activity of FabG after 120 min of incubation. However, the same effect was achieved in only 20 min when the concentration of EGCG was 600 μ mol/L (Li et al.¹⁴). In the present results, CTs decreased the activity of FabG by 65.95% compared with the control after 2 h of incubation and decreased the activity of FabG by 37.55% compared with the control after 6 h. However, FabI (coded by PEPE_RS04200) was up-regulated in the CT-treated group. FabI is involved in acyl-ACP

synthesis, which mainly produces phospholipids and is the last step of fatty acid synthesis. This protein was up-regulated in *P. acidilactici* in response to acid stress, which resulted in wrinkling, tiny pores, and the partial collapse of cells.¹⁹ The present results showed that CTs damaged the cell wall and membrane, in accordance with the effects of acid stress on *P. acidilactici*. Thus, the up-regulated expression of FabI in *P. pentosaceus* SF11 was probably mainly in response to cell wall and membrane damage under CT treatment. Furthermore, the AcpS protein coded by PEPE_RS07575 is described as a holoacyl carrier protein (ACP) synthase. This enzyme is involved in the production of active holo-ACPs, which are an important component in the type II fatty acid synthase of bacteria.³⁵ Thus, the present results suggested that CTs could inhibit the fatty acid synthesis system through directly decreasing the activity of some enzymes and down-regulating their expression. The ChrR protein coded by PEPE_RS06535 is described as a NAD(P)H-dependent oxidoreductase. The ChrR protein is a soluble quinone reductase contained in most bacteria and has a much greater affinity for a variety of quinone substrates, such as benzoquinone and duroquinone.³⁶ Considering that the B ring of EGC showed capacity to autooxidation that results in orthoquinone production,^{4,6} this indicates that *P. pentosaceus* SF11 may have ability to reduce quinone. However, the present findings showed that the ChrR protein disappeared under CT exposure. The expression of ChrR is up-regulated in response to H₂O₂ stress; this enzyme can protect cells against oxidative stress via generating reduced quinols to quench reactive oxygen species (ROS).³⁶ Previous research found that the intracellular ROS level of *P. pentosaceus* SF11 increased under CT exposure, and the H₂O₂ content increased after 24 h of incubation (our former study, data are not shown). Therefore, this result was mainly due to the lack of ChrR protein expression in *P. pentosaceus* SF11 after CT treatment, but the mechanism needs further study. In addition, the OhrR protein coded by PEPE_RS08520 belongs to the multiple antibiotic resistance regulator (MarR) family as a winged helix-turn-helix transcriptional regulator. The expression of organic hydroperoxide resistance regulator (OhrR) protein in bacteria is mainly up-regulated in response to oxidative stress caused by organic hydroperoxides (OHPs).³⁷ The OhrR protein disappeared after CT treatment, indicating that oxidative stress was only attributed to H₂O₂ by CTs generated. The FtsK protein coded by PEPE_RS03355 is described as a DNA translocase. FtsK is a membrane-bound enzyme involved in the final stages of bacterial chromosome segregation, and the lack of this enzyme will prevent chromosome segregation and lead to cell death.³⁸ The present study suggests that CTs could inhibit cell division via the decreased expression of enzymes for chromosome segregation. The MiaA protein coded by PEPE_RS03600 is described as tRNA (adenosine(37)-N6)-isopentenyltransferase. MiaA is involved in hypermodified nucleoside synthesis at the 3'-adjacent adenosine (A₃₇), which is essential for efficient and highly accurate protein translation by the bacterial ribosome.³⁹ Thus, the present findings indicated that CTs could disturb the protein translation of bacteria through decreased expression of essential enzymes. The MsrC protein coded by PEPE_RS06280 is described as a GAGA transcription factor (GAF) domain-containing protein. The *msrC* genes share a high degree of similarity with the bacterial erythromycin resistance determinant *msr* (A), and the protein coded by these genes could enhance bacterial resistance against erythromycin.⁴⁰ Thus, the present results

suggest that CTs could decrease the resistance of *P. pentosaceus* SF11 against drugs. EGCG showed synergistic activity with β -lactams, which was attributed to the inhibition of penicillin-binding proteins (PBPs), such as PBP2 and PBP3, by EGCG.⁶ The different mechanisms between CTs and EGCG probably showed that among these proteins involved in drug resistance CTs derived from sainfoin could directly decrease protein expression, while EGCG from tea only inhibited protein activity. The AqpZ protein coded by PEPE_RS06045 is described as an aquaporin family protein. Bacteria such as *E. coli* contain two aquaporins (GLpF and AqpZ), among which AqpZ is the most efficient water channel.⁴¹ The results of the present study probably suggest that CTs damage cell membrane permeability due to the impact of CTs on the water channel transport system.

5. CONCLUSIONS

The MIC of CTs against *P. pentosaceus* SF11 was 1500 mg/L, and the bacterial count after CT treatment was reduced by only 8%, indicating that CTs is a bacteriostatic agent. Proteomic analysis revealed that 40.80% of proteins showed significant differences in expression between the CT treatment and the control. Among these DEPs, 81.58% were down-regulated after CT treatment ($p < 0.05$). The expression of the most important proteins (30 proteins) was not strongly influenced by CTs ($\log_2\text{FCI} < 2$), and these proteins were most involved in LTA synthesis, peptidoglycan synthesis, and glycine metabolism, which could partly explain why CTs acted as a bacteriostatic agent rather than a bactericidal agent. Twenty-seven proteins were not detected due to the impact of CTs. These proteins were involved in functions including fatty acid synthesis, RNA synthesis and translation, drug resistance, and cell membrane permeability. Therefore, the results of this study suggest that the inhibition mechanism of CTs is related to cell membrane damage and the inhibition of cell reproduction.

■ ASSOCIATED CONTENT

Data Availability Statement

The mass spectrometry proteomics data have been deposited to the ProteomeXchange Consortium (<http://proteomecentral.proteomexchange.org>) via the iProX partner repository with the data set identifier PXD045431 (accessed on 18 September 16, 2023).

SI Supporting Information

The Supporting Information is available free of charge at <https://pubs.acs.org/doi/10.1021/acsomega.3c08947>.

Methods and results for this research, strain isolation and CT extraction, enzyme activity analysis of intracellular protease, intracellular concentration of ATP analysis, proteomic analysis, and parallel reaction monitoring (PRM) analysis, CT composition, top 30 important proteins, 20 DEPs for PRM analysis, 27 proteins which were undetected after CT treated, results of DEPs for PRM analysis, interaction networks of protein, top 30 DEPs (in proteins interaction networks) involved in pathways, intracellular content of ATP and activity of DHFR (PDF)

AUTHOR INFORMATION

Corresponding Author

Chunhui Ma – Grassland Science, School of Animal Technology, Shihezi University, Shihezi 832000, China;
Email: chunhuima@126.com

Authors

Rongzheng Huang – Grassland Science, School of Animal Technology, Shihezi University, Shihezi 832000, China;
orcid.org/0000-0001-6684-1791

Fanfan Zhang – Grassland Science, School of Animal Technology, Shihezi University, Shihezi 832000, China

Xuzhe Wang – Grassland Science, School of Animal Technology, Shihezi University, Shihezi 832000, China

Fan Yang – Grassland Science, School of Animal Technology, Shihezi University, Shihezi 832000, China

Complete contact information is available at:

<https://pubs.acs.org/10.1021/acsomega.3c08947>

Author Contributions

R.H.: conceptualization, writing-original draft, data curation, investigation, and methodology. C.M.: supervision, project administration, and funding acquisition. F.Z.: review and editing and supervision. F.Z.: review and editing. X.W.: formal analysis and software. F.Y.: software.

Funding

This work was supported by the National Natural Science Foundation of China (NSFC) [Grant Number 32060399] and the China Agriculture Research System of MOF and MARA [Grant Number CARS].

Notes

The authors declare no competing financial interest.

REFERENCES

- (1) Rodriguez, A. V.; de Nadra, M. C. M. Effect of pH and Hydrogen-Peroxide Produced by *Lactobacillus Hilgrdii* on *Pediococcus Pentosaceus* Growth. *FEMS Microbiol. Lett.* **1995**, *128* (1), 59–62.
- (2) Jiang, S. M.; Cai, L. Z.; Lv, L. X.; Li, L. J. *Pediococcus Pentosaceus*, a Future Acidic or Probiotic Candidate. *Microbial Cell Factories* **2021**, *20* (1), 45.
- (3) Huang, R. Z.; Zhang, F. F.; Wang, T.; Zhang, Y. L.; Li, X.; Chen, Y. C.; Ma, C. H. Effect of Intrinsic Tannins on the Fermentation Quality and Associated with the Bacterial and Fungal Community of Sainfoin Silage. *Microorganisms* **2022**, *10* (5), 844.
- (4) Zeller, W. E. Activity, Purification, and Analysis of Condensed Tannins: Current State of Affairs and Future Endeavors. *Crop Science* **2019**, *59* (13), 886–904.
- (5) Ikigai, H.; Nakae, T.; Hara, Y.; Shimamura, T. Bactericidal Catechins Damage the Lipid Bilayer. *Biochimica et biophysica acta* **1993**, *1147* (1), 132–136.
- (6) Renzetti, A.; Betts, J. W.; Fukumoto, K.; Rutherford, R. N. Antibacterial Green Tea Catechins from a Molecular Perspective: Mechanisms of Action and Structure-Activity Relationships. *Food and Function* **2020**, *11* (11), 9370–9396.
- (7) Arakawa, H.; Maeda, M.; Okubo, S.; Shimamura, T. Role of Hydrogen Peroxide in Bactericidal Action of Catechin. *Biol. Pharm. Bull.* **2004**, *27* (3), 227–281.
- (8) Wiegand, I.; Hilpert, K.; Hancock, R. E. W. Agar and Broth Dilution Methods to Determine the Minimal Inhibitory Concentration (MIC) of Antimicrobial Substances. *Nat. Protoc.* **2008**, *3* (2), 163–175.
- (9) Xu, Y. F.; Shi, C.; Wu, Q.; Zheng, Z. W.; Liu, P. F.; Li, G. H.; Peng, X. L.; Xia, X. D. Antimicrobial Activity of Punicalagin Against *Staphylococcus Aureus* and Its Effect on Biofilm Formation. *Foodborne Pathogens and Disease* **2017**, *14* (5), 282–287.
- (10) Tanaka, K.; Komiyama, A.; Sonomoto, K.; Ishizaki, A.; Hall, S. J.; Stanbury, R. Two Different Pathways for D-Xylose Metabolism and the Effect of Xylose Concentration on the Yield Coefficient of L-Lactate in Mixed-Acid Fermentation by the Lactic Acid Bacterium *Lactococcus Lactis* IO-1. *Appl. Microbiol. Biotechnol.* **2002**, *60* (1–2), 160–167.
- (11) Bradford, M. A Rapid and Sensitive Method for the Quantitation of Microgram Quantities of Protein Utilizing the Principle of Protein-Dye Binding. *Anal. Biochem.* **1976**, *72*, 248–254.
- (12) Deng, L. S.; Sundriyal, S.; Rubio, V.; Shi, Z. Z.; Song, Y. C. Coordination Chemistry Based Approach to Lipophilic Inhibitors of 1-Deoxy-D-Xylulose-5-Phosphate Reductoisomerase. *J. Med. Chem.* **2009**, *52* (21), 6539–6542.
- (13) Heath, R. J.; Rock, C. O. Regulation of Malonyl-CoA Metabolism by Acyl-Acyl Carrier Protein and Beta-Ketoacyl-Acyl Carrier Protein Synthases in *Escherichia Coli*. *J. Biol. Chem.* **1995**, *270* (26), 15531–15538.
- (14) Li, B. H.; Zhang, R.; Du, Y.-T.; Sun, Y.-H.; Tian, W. X. Inactivation Mechanism of the Beta-Ketoacyl-[Acyl Carrier Protein] Reductase of Bacterial Type-II Fatty Acid Synthase by Epigallocatechin Gallate. *Biochem. Cell Biol.* **2006**, *84* (5), 755–762.
- (15) Yi, S. M.; Zhu, J. L.; Fu, L. L.; Li, J. R. Tea Polyphenols Inhibit *Pseudomonas Aeruginosa* through Damage to the Cell Membrane. *Int. J. Food Microbiol.* **2010**, *144* (1), 111–117.
- (16) Xiong, L.-G.; Chen, Y.-J.; Tong, J.-W.; Huang, J.-A.; Li, J.; Gong, Y.-S.; Liu, Z.-H. Tea Polyphenol Epigallocatechin Gallate Inhibits *Escherichia Coli* by Increasing Endogenous Oxidative Stress. *Food Chem.* **2017**, *217*, 196–204.
- (17) Yoshihara, E.; Nakae, T. Cytolytic Activity of Liposomes Containing Stearylamine. *Biochimica et biophysica acta* **1986**, *854* (1), 93–101.
- (18) Bae, H. D.; McAllister, T. A.; Yanke, J.; Cheng, K.; Muir, A. Effects of Condensed Tannins on Endoglucanase Activity and Filter Paper Digestion by *Fibrobacter Succinogenes* S85. *Appl. Environ. Microbiol.* **1993**, *59* (7), 2132–2138.
- (19) Zhang, M. H.; Wu, N.; Fan, Y. Q.; Xu, C. Y.; Luo, J. M.; Wang, Y. X.; Yu, K. H.; Wang, M. Proteomic Profiling and Stress Response in *Pediococcus Acidilactici* under Acetic Acid. *J. Agric. Food Chem.* **2022**, *70* (39), 12708–12721.
- (20) Nie, R. Z.; Dang, M. Z.; Ge, Z.-z.; Huo, Y.-q.; Yu, B.; Tang, S. W. Influence of the Gallate Moiety on the Interactions between Green Tea Polyphenols and Lipid Membranes Elucidated by Molecular Dynamics Simulations. *Biophys. Chem.* **2021**, *274*, No. 106592.
- (21) Li, H. H.; Mei, X. X.; Liu, B.; Li, Z.; Wang, B.; Ren, N.; Xing, D. F. Insights on Acetate-Ethanol Fermentation by Hydrogen-Producing Ethanoligenens under Acetic Acid Accumulation Based on Quantitative Proteomics. *Environ. Int.* **2019**, *129*, 1–9.
- (22) Neuhaus, F. C.; Baddiley, J. A Continuum of Anionic Charge: Structures and Functions of D-Alanyl-Teichoic Acids in Gram-Positive Bacteria. *Microbiology and Molecular Biology Reviews* **2003**, *67* (4), 686–723.
- (23) Araki, Y.; Ito, E. Linkage Units in Cell Walls of Gram-Positive Bacteria. *Critical Reviews in Microbiology* **1989**, *17* (2), 121–135.
- (24) Shetty, S.; Varshney, U. Regulation of Translation by One-Carbon Metabolism in Bacteria and Eukaryotic Organelles. *J. Biol. Chem.* **2021**, *296*, 100088.
- (25) Mandelbaum-Shavit, F.; Grossowicz, N. Dihydrofolate Reductase in *Pediococcus Cerevisiae* Strains Susceptible and Resistant to Amethopterin. *Antimicrob. Agents Chemother.* **1974**, *6* (3), 369–371.
- (26) Navarro-Martínez, M. D.; Navarro-Perán, E.; Cabezas-Herrera, J.; Ruiz-Gómez, J.; García-Cánovas, F.; Rodríguez-López, J. N. Antifolate Activity of Epigallocatechin Gallate against *Stenotrophomonas Maltophilia*. *Antimicrob. Agents Chemother.* **2005**, *49* (7), 2914–2920.
- (27) Sánchez-del-Campo, L.; Sáez-Ayala, M.; Chazarra, S.; Cabezas-Herrera, J.; Rodríguez-López, J. N. Binding of Natural and Synthetic

Polyphenols to Human Dihydrofolate Reductase. *Int. J. Mol. Sci.* **2009**, *10* (12), 5398–5410.

(28) Raju, A.; Degani, M. S.; Khambete, M. P.; Ray, M. K.; Rajan, M. G. R. Antifolate Activity of Plant Polyphenols against Mycobacterium Tuberculosis. *Phytotherapy Research* **2015**, *29* (10), 1646–1651.

(29) Mora, D.; Parini, C.; Fortina, M. G.; Manachini. Multilocus Hybridization Typing in *Pediococcus Acidilactici* Strains. *Curr. Microbiol.* **2002**, *44* (2), 77–80.

(30) Shi, J.; Wang, Y. Z.; Wei, H. R.; Hu, J. J.; Gao, M. T. Structure Analysis of Condensed Tannin from Rice Straw and Its Inhibitory Effect on Staphylococcus Aureus. *Industrial Crops and Products* **2020**, *145*, No. 112130.

(31) Perez-Gil, J.; Rodriguez-Concepcion, M. Metabolic Plasticity for Isoprenoid Biosynthesis in Bacteria. *Biochem. J.* **2013**, *452*, 19–25.

(32) Kuzuyama, T.; Takahashi, S.; Watanabe, H.; Seto, H. Direct Formation of 2-C-Methyl-D-Erythritol 4-Phosphate from 1-Deoxy-D-Xylulose 5-Phosphate by 1-Deoxy-D-Xylulose 5-Phosphate Reductoisomerase, a New Enzyme in the Non-Mevalonate Pathway to Isopentenyl Diphosphate. *Tetrahedron Lett.* **1998**, *39* (24), 4509–4512.

(33) Eisenreich, W.; Rohdich, F.; Bacher, A. Deoxyxylulose Phosphate Pathway to Terpenoids. *Trends in Plant Science* **2001**, *6* (2), 78–84.

(34) Hui, X.; Liu, H.; Tian, F. L.; Li, F. F.; Li, H.; Gao, W. Y. Inhibition of Green Tea and the Catechins against 1-Deoxy-D-Xylulose 5-Phosphate Reductoisomerase, the Key Enzyme of the MEP Terpenoid Biosynthetic Pathway. *Fitoterapia* **2016**, *113*, 80–84.

(35) Tropf, S.; Revell, W. P.; Bibb, M. J.; Hopwood, D. A.; Schweizer, M. Heterologously Expressed Acyl Carrier Protein Domain of Rat Fatty Acid Synthase Functions in Escherichia Coli Fatty Acid Synthase and Streptomyces Coelicolor Polyketide Synthase Systems. *Chem. Biol.* **1998**, *5* (3), 135–146.

(36) Gonzalez, C. F.; Ackerley, D. F.; Lynch, S. V.; Martin, A. ChrR, a Soluble Quinone Reductase of Pseudomonas Putida That Defends against H₂O₂. *J. Biol. Chem.* **2005**, *280* (24), 22590–22595.

(37) Kim, H.; Choe, J. The X-Ray Crystal Structure of PA1374 from Pseudomonas Aeruginosa, a Putative Oxidative-Stress Sensing Transcriptional Regulator. *Biochem. Biophys. Res. Commun.* **2013**, *431* (3), 376–381.

(38) Lee, J. Y.; Finkelstein, I. J.; Crozat, E.; Sherratt, D. J.; Greene, E. C. Single-Molecule Imaging of DNA Curtains Reveals Mechanisms of KOPS Sequence Targeting by the DNA Translocase FtsK. *Proceedings of The National Academy of Sciences of The United States of America* **2012**, *109* (17), 6531–6536.

(39) Chimnarong, S.; Forouhar, F.; Sakai, J.; Yao, M.; Tron, C. M.; Atta, M.; Fontecave, M.; Hunt, J. F.; Tanaka, I. Snapshots of Dynamics in Synthesizing N⁶-Isopentenyladenosine at the tRNA Anticodon. *Biochemistry* **2009**, *48* (23), 5057–5065.

(40) Reynolds, E.; Cove, J. H. Enhanced Resistance to Erythromycin Is Conferred by the Enterococcal msrC Determinant in Staphylococcus Aureus. *J. Antimicrob. Chemother.* **2005**, *55* (2), 260–264.

(41) Savage, D. F.; Egea, P. F.; Robles-Colmenares, Y.; O'Connell, J. D.; Stroud, R. M. Architecture and Selectivity in Aquaporins: 2.5 Å X-Ray Structure of Aquaporin Z. *PLoS Biol.* **2003**, *1* (3), No. e72.